Classification of LPI Radar Signals Using Spectral Correlation and Support Vector Machines

Thomas Schucker, and Garrett Vanhoy
Dept. of Electrical and Computer Engineering
The University of Arizona
Tucson, AZ 85721-0104
{tschucker, gvanhoy}@email.arizona.edu

***Abstract*—In modern radar systems, low probability of intercept (LPI) waveforms are used to make detection by a potential adversary difficult. This is accomplished using wideband waveforms, frequency hopping, and continuous waveforms (FMCW) to reduce the signal profile. The low signal profile of the LPI signal enables the radar to perform detection and or target tracking while the target remains unaware. Several modulation techniques such as polytime codes, polyphase codes, FSK, and FMCW are used to produce LPI signals for transmission. From the target side, the incoming LPI signal is wideband with unknown center frequency, and low SNR. This paper looks at the ability of spectral correlation along with a support vector machine (SVM) in order to automatically classify the different LPI signal types in a non-cooperative environment.**

***Index Terms*—Low probability of intercept, Support vector machines, Spectral correlation, Radar signals**

I. Introduction

The initial development of radar technology was driven by its ability to provide a tactical advantage by providing information on the location and movement of targets at distances beyond the range of the naked eye. This allowed risky surveillance and reconnaissance missions to be done completely without the target's awareness. One major caveat to the use of radar is that the transmitted pulse can be intercepted by a target and used to locate the radar source, thus neutralizing the advantage of stealth. For this reason, modern radars employ what is known a low probability of intercept (LPI) waveforms that are difficult for an intercept radio to detect. A typical scenario for the use of an LPI radar system is seen by Figure 1 where the LPI radar has a range at which a target can be detected of R_t. The intercept receiver has a range at which a transmitted pulse can be intercepted of R_i. R_t is typically an order of magnitude larger than R_i so that targets can be detected without interception. LPI waveforms accomplish this by using wide bandwidths, continuous waveforms rather than pulsed waveforms, frequency hopping patterns, and narrow radiation patterns. All of these contribute to viable waveforms that are difficult to intercept. [1] LPI signals provide other benefits in addition to being difficult to detect, and so their use is not limited to military applications. These benefits include high range resolution detection for short range applications, low transmit power, and lower cost compared to solid state components.

In [1] several different methods are used to classify LPI radar waveforms. These methods generally involve time-frequency analysis with the Wigner-Ville distribution, Choi-Williams distribution, or quadrature mirror filter banks. Work in each of [2]–[4] employs one of more of these analysis tools in conjunction with neural networks to achieve classification. Modulation classification for communications signals has received more attention in the literature than radar signal classification, but much of the work in this field can be extended to radar signal classification even though their objectives are markedly different [5]. In this work, spectral correlation and support vector machines, which are the mechanisms behind the signal classification methods in [6], [7], will provide the basis for our approach to LPI radar signal classification. The use of spectral correlation density (SCD) has been instrumental in a variety of signal processing and classification tasks in communications, radar, and others [8]–[11]. This tems primarily stems from its ability to detect and characterize the presence of periodic features, such as pulse repetition frequency or carrier frequency, even in the presence of noise and other channel effects.

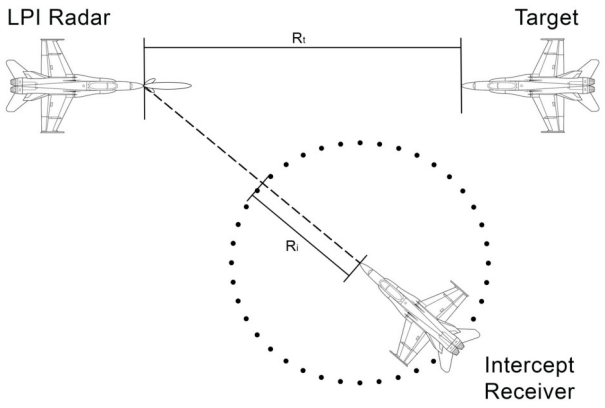

Fig. 1. LPI Radar Scenario

In Section II the models and assumptions are summarized. In Section III we provide a theoretical background for the SCD and its use. In Section IV we show the results of our classification method on 12 different LPI signals and finally conclude in Section V.

II. Models

For LPI waveforms, the bandwidth, frequency hopping pattern, or pulse duration are not known *a-priori* to the intercept receiver, making detection much more difficult than for the LPI radar. With these characteristics, it is a necessary assumption for both detection and classification that the intercept radar meet a minimum level of operating characteristics, such as receiver bandwidth, memory size, and computational resources. It is important to note that detection is a necessary condition before classification can even be considered and the latter is definitely a difficult task. However, the primary contribution of this work is to reveal the minimum operating requirements in a detector that enable this classification. Therefore, it is assumed that the signal has been detected and its center frequency and bandwidth are known within a margin of error of ten percent.

There are a few families of LPI signals on which this work will focus. The first is the traditional frequency modulated continuous wave (FMCW), which is based on modulating the frequency of the transmitted signal in a linear or non-linear fashion. The next type of signal is the polyphase signal, where the phase of a sinusoidal signal is modulated to produce a pulse compression waveform. The polyphase codes that determine the phase are based on approximations to stepped frequency or linear frequency (LFM) waveforms. Polytime signals are similar to the polyphase signals in that they are generated by the modulation of a sinusoid's phase, but do this by varying the time spent at each phase state. There are several other type of LPI signals that are included, such as frequency shift keying and frequency hopping waveforms. A more detailed description for each of these LPI signals can be found in [1].

A. Frequency Modulated Continuous Wave

The first type of radar waveforms are Frequency Modulated Continuous Waves (FMCW). There are two types of FMCW signals that will be generated, the basic sawtooth wave, and the more useful triangular wave.

1) Sawtooth: The sawtooth waveform is a repetitious LFM signal which can be described by:

$$s_1(t) = \sin 2\pi \left[\left(f_c - \frac{B}{2} \right) t + \frac{B}{2T_p} t^2 \right], \tag{1}$$

where f_c is the carrier frequency, B is the bandwidth, and T_p is the pulse duration. This signal can be generated to have very large bandwidths while remaining easy for the radar to process.

2) Triangular: The triangular wave is also based on the LFM waveform. This allows the radar to resolve the range and speed of multiple targets. The triangular wave keeps the same beneficial aspects of the sawtooth waves described by equation (1) and is described by:

$$s_2(t) = \sin 2\pi \left[\left(f_c + \frac{B}{2} \right) t - \frac{B}{2T_p} t^2 \right]. \tag{2}$$

In the case of the triangular wave the duration of a pulse will be $2T_p$, this is because the equation (1) and equation (2) are concatenated one after the other in order to produce the increasing frequency and decreasing frequency components.

B. Polyphase Codes

The polyphase signal is generated from a sequence of discrete phase values which is the signal's polyphase code. The polyphase code is derived by approximating a stepped frequency or LFM waveform. The number of phase steps are determined by the waveform they are trying to approximate. Once the polyphase code is determined it is used to modulate the phase of a sinusoidal continuous wave signal by incrementing the phase state for each time step. The codes implemented will be the Frank, P1, P2, P3, and P4 codes described in the following sections.

1) Frank: The Frank code is of the first type of polyphase codes which are derived from a step approximation to a LFM waveform using M frequency steps and M samples per frequency. The number of phases in the Frank code are $N_c = M^2$ with each phase based on the i^{th} sample from $i = 1, 2, \ldots, M$ of the j^{th} frequency from $j = 1, 2, \ldots, M$.

$$\phi_k = \phi_{i,j} = \frac{2\pi}{M}(i-1)(j-1) \tag{3}$$

2) P1: The P1 code is similar to the Frank code in that its length is $N_c = M^2$ but it derives the phases differently from the stepped approximation to the LFM by using double sideband detection.

$$\phi_k = \phi_{i,j} = \frac{-\pi}{M}[M - (2j-1)][(j-1)M + (i-1)] \tag{4}$$

3) P2: The P2 code has the same phase increment within each phase group as the P1 code but its starting phase is different. For the P2 code M must be even $M = 2, 4, 6, \ldots$, this is because the code was derived with the desire for low autocorrelation sidelobes .

$$\phi_k = \phi_{i,j} = \frac{-\pi}{2M}[2i - 1 - M][2j - 1 - M] \tag{5}$$

4) P3: The P3 code differs from the previous polyphase codes by not approximating the LFM waveform from a stepped frequency but instead converting it to baseband using single sideband detection. The phase for the k^{th} sample is shown by equation (6) where $k = 1, 2, \ldots, N_c$.

$$\phi_k = \frac{\pi}{N_c}(k-1)^2 \tag{6}$$

5) P4: The P4 code is derived similarly to the P3 code but uses coherent double sideband detection to determine the phase states. The phase for the k^{th} sample is shown by equation (7) where $k = 1, 2, \ldots, N_c$.

$$\phi_k = \frac{\pi}{N_c}(k-1)^2 - \pi(k-1) \tag{7}$$

C. Polytime Codes

The polytime signals are similar to the polyphase signals in that they are generated from a code which approximates a stepped or LFM waveform. In the case of polytime codes their are a fixed number of phase states and the time spent at each state is varied over the duration of the code period. The codes implemented will be the T1, T2, T3, and T4 codes described below.

1) T1(n): The T1(n) code is generated by the approximation of the stepped frequency waveform where the leading segment is zero. Equation (8) describes the wrapped phase versus time of the T1(n) code as:

$$\phi_{T1}(t) = \mod\left\{\frac{2\pi}{n}\left\lfloor(kt - jt)\frac{jn}{T}\right\rfloor, 2\pi\right\}, \tag{8}$$

where k is the number of segments in the T1(n) code, n is the number of phase states, $j = 0, 1, 2, \ldots, k-1$ is the segment number in the stepped frequency waveform, T is the code period, t is time and $\lfloor \ldots \rfloor$ is the floor operator.

2) T2(n): The T2(n) code is generated similarly to the T1(n) code by approximating the stepped frequency waveform, but approximates one that is zero at its center frequency. When using an odd number of segments k the zero frequency is the center segment, and when k is even the zero frequency will be between the two segments at the center. equation (9) describes the wrapped phase of the T2(n) code as:

$$\phi_{T2}(t) = \mod\left\{\frac{2\pi}{n}\left\lfloor(kt - jt)\frac{2j-k+1}{T}\frac{n}{2}\right\rfloor, 2\pi\right\}. \tag{9}$$

3) T3(n): The T3(n) code is generated differently than the previous two polytime codes. The T3(n) code is generated by approximating a LFM waveform that is zero beat at its leading edge instead of using the stepped frequency waveform.

$$\phi_{T3}(t) = \mod\left\{\frac{2\pi}{n}\left\lfloor\frac{nBt^2}{2T_p}\right\rfloor, 2\pi\right\} \tag{10}$$

Equation (10) describes the wrapped phase of the T3(n) code, where B is the modulation bandwidth and T_p is the period for modulation.

4) T4(n): The T4(n) code is generated conceptually similar to the T3(n) code but approximates a LFM waveform which is zero at its center frequency. Equation (11) describes the wrapped phase of the T4(n) code.

$$\phi_{T4}(t) = \mod\left\{\frac{2\pi}{n}\left\lfloor\frac{nBt^2}{2T_p} - \frac{nBt}{2}\right\rfloor, 2\pi\right\} \tag{11}$$

D. Frequency-Hopping Radar

As opposed to the linear FMCW, radar frequency hopping radar techniques utilize a set of frequencies that it changes to in a random fashion impairing the ability of an intercept receiver to intercept and jam the signal. While moving the signal does not decrease the signal profile like FMCW or phase modulation enabling a higher rate of detection, it significantly decreases the chance of interception, allowing it to be classified as an LPI signal.

1) FSK: In FSK radar a transmitted frequency is chosen from a frequency hopping sequence with frequencies $\{f_1, f_2, \ldots, f_N\}$, then it is transmitted for a corresponding time period $\{t_1, t_2, \ldots, t_N\}$. For a continuous wave FSK radar the transmitted complex signal will have the form:

$$s(t) = \cos(2\pi f_j t), \tag{12}$$

where $i = 1, 2, \ldots, N$.

2) Costas Frequency Hopping: The Costas code is a frequency hopping scheme used in radar to provide unambiguous range and Doppler measurements. It follows a sequence of frequencies $f_1, \ldots, f_N$ which will be a permutation of the integers $1, \ldots, N$. The permutation of the integers is governed by:

$$f_{k+i} - f_k \neq f_{j+i} - f_j, \tag{13}$$

for i, j, and k such that $1 \leq k < i < i+j \leq N$. An example of this sequence being $f_i = \{2, 4, 8, 5, 10, 9, 7, 3, 6, 1\}kHz$.

III. Theory of SCD

A stochastic process $x(t)$ whose mean and autocorrelation function, $R_x(\tau) = \int_{-\infty}^{\infty} x(t - \frac{\tau}{2})x(t + \frac{\tau}{2})dt$, are periodic is said to be wide-sense cyclostationary. Due to this periodicity, a Fourier series whose coefficients are $R_x(\alpha, \tau)$ are sufficient to describe the cyclic autocorrelation function (CAF) of the process. It is well known that the power spectral density (PSD) is related to the Fourier transform of the autocorrelation function. Then the Wiener relationship, which relates the power spectral density (PSD) to the autocorrelation function by Fourier transform, can be used to describe the SCD:

$$S_x(\alpha, f) = \int_{-\infty}^{\infty} R_x(\alpha, \tau)e^{-j2\pi f\tau}d\tau. \tag{14}$$

Peaks in the SCD describe correlation in time between each pair of frequencies in the PSD. Naturally, this gives the SCD the ability to identify and characterize underlying periodicities of the signal. Each LPI signal contains unique periodicities that can be used to classify them and these have been well-documented in [1]. The SCD is also granted a level of noise immunity because there are no inherent periodicities in noise. Thus, one might think of noise as spreading energy across all possible periodicities evenly.

For a digital signal, estimating the SCD has two commonly-used methods which are optimized for computational efficiency. They are called FFT Accumulation Method (FAM) and Strip Spectral Correlation (SSC). The FAM is the most efficient computationally and is calculated as follows:

$$X_{N'}(n, k) = \sum_{r=-N'/2}^{r=N'/2} a[r]x[n - r]e^{-j2\pi k(n-r)T_s} \tag{15}$$

$$S_x^{\alpha}(n, k) = \frac{1}{N}\sum_{n=0}^{N-1}\frac{1}{N'}X_{N'}\left(n, k + \frac{\alpha}{2}\right)X_{N'}^{*}\left(n, k - \frac{\alpha}{2}\right) \tag{16}$$

where N' and N together determine a resolution in both the time and frequency domains and $a[n]$ is an arbitrary windowing function. Equation (15) is the sliding window discrete Fourier transform (DFT) with window $a[n]$. For this work $N' = 256$, $N = 32$, and $a[n]$ is a hamming window of length N'. The SCD estimate also contains some symmetries which we leverage to make estimation even more computationally efficient. These identities are noted in [12]:

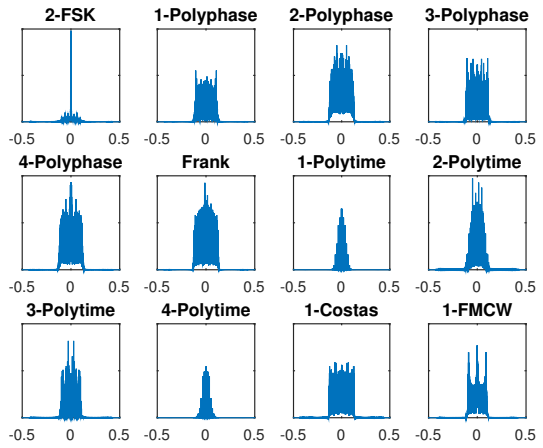

Fig. 2. Alpha Profiles of LPI Signals

$$\hat{S}_x^{\alpha}(f) = \hat{S}_x^{-\alpha}(f)^* \tag{17}$$

$$\hat{S}_x^{\alpha}(f) = \hat{S}_x^{\alpha}(-f) \tag{18}$$

The SCD itself contains enough information to determine particular properties of each signal, however it contains far too many points to be used directly for classification and the number of points is significantly cut down by looking at generic features. First, the $|S_x^{\alpha}(f)|$ is sufficient for classification, therefore the identities in (18) allow for the estimation of only one quadrant of the SCD. Second, the location of the peaks is unique enough to examine a flattened version of the SCD. The maximum of the SCD along the α axis is taken to create an $\alpha-$profile which contains significantly less points. The $\alpha-$profile for each signal of interest is shown in Figure 2.

It is clear from this figure that indeed, the SCD is symmetric on the α axis and thus only half of it is necessary for classification. Lastly, among the points in the $\alpha-$profile, only a few points are unique to each signal and should be used for classification. Determining which of these points are good in the use of classifiers can be done using the LASSO algorithm which is implemented in MATLAB [13]. Ultimately, this reduces the number of elements use from the original SCD to a feature vector of less than 100 points.

Finally, a support vector machine is trained using the "example" feature vectors for each signal in a process called supervised learning. Support vector machines (SVMs) can be used for this type of data. Support vector machines were first introduced by Boser et al [14] in 1992. It has had successful applications in many fields that involve classification and fits into the broader study of supervised learning models. SVM is a learning algorithm that is widely used due to its ability to deal with high-dimensional data and efficiency in modeling diverse data. As a supervised learning algorithm an SVM is constructed offline by using a set of training data. It uses the training data to construct a hyperplane that optimally separates each class. This is sufficient only for linearly separable patterns, but can be extended to other patterns by transformations of the data.

TABLE I
CONFUSION MATRIX FOR -5 DB SNR

	2FSK	P1	P2	P3	P4	Frank	T1	T2	T3	T4	Costas	FMCW
2FSK	47	0	0	0	0	0	0	0	0	0	0	0
P1	0	10	7	4	3	8	4	2	6	4	1	1
P2	0	2	8	5	8	7	2	2	7	7	0	0
P3	1	0	12	10	3	7	0	1	2	10	1	1
P4	0	6	9	5	5	8	4	0	6	9	1	0
Frank	0	3	12	4	3	9	5	0	4	9	0	0
T1	0	3	7	4	5	8	20	0	1	2	0	0
T2	0	1	3	7	1	5	4	18	3	2	0	0
T3	0	5	10	4	4	5	1	2	6	9	2	0
T4	0	5	2	4	6	7	5	2	5	17	1	0
Costas	0	7	8	5	3	3	2	2	4	1	16	0
FMCW	0	0	9	1	2	1	2	0	3	2	1	28

TABLE II
CONFUSION MATRIX FOR 10 DB SNR

	2FSK	P1	P2	P3	P4	Frank	T1	T2	T3	T4	Costas	FMCW
2FSK	47	0	0	0	0	0	0	0	0	0	0	0
P1	0	36	0	0	0	0	0	0	0	1	3	12
P2	0	0	32	0	0	0	0	0	0	3	4	0
P3	0	0	0	21	0	0	0	0	0	12	5	7
P4	0	0	0	0	12	0	0	3	0	13	15	10
Frank	0	0	0	0	0	10	0	1	0	9	2	20
T1	0	0	0	0	0	0	46	0	0	0	2	0
T2	0	0	0	0	0	0	0	51	0	0	0	0
T3	0	0	0	0	0	0	1	0	32	2	5	0
T4	0	0	0	0	0	0	1	1	2	51	0	0
Costas	0	0	0	0	0	0	0	0	0	0	51	1
FMCW	0	0	0	0	0	0	0	0	0	0	0	56

IV. CLASSIFICATION AND RESULTS

Each of the LPI signals of interest were generated in MATLAB with the addition of white Gaussian noise so as to create a range of SNRs between -5 and 10 dB. Then, the SVM is trained on half of the generate feature vectors chosen at random. Finally, the SVM is used to classify the remaining feature vectors to evaluate the performance of classification. The results of classification can be generally described in two ways. First, a confusion matrix where the columns are the input or *actual* modulation and the rows are the output or *predicted* modulation.

The results for classification with each signal having -5 dB SNR and 10 dB SNR in additive white Gaussian noise are tabulated in Table I and II respectively. Among the signals of interest, the Frank code is the most difficult to differentiate from the others. Looking at Table I, although the Frank code is being transmitted is being classified as the P1, P2, and P3 codes 3, 12, and 4 times respectively. Correctly classifying this code can be found by value of the gray box in the Frank code row by the sum of all of the values in the Frank code row. This misclassification is partially alleviated in higher SNRs according to Table II where although the Frank code is being transmitted, it is only classified as T2, T4, and Costas 1, 9, and 2 times respectively. The overall results for all trials along the entire range of SNRs are tabulated in Table III. Overall, the signal that is most accurately classified is the 2-FSK signal. This is because the FSK signal has the most unique $\alpha-$profile of all of the signals such that even noise

TABLE III
CONFUSION MATRIX FOR -5 TO 10 DB SNR

	2FSK	P1	P2	P3	P4	Frank	T1	T2	T3	T4	Costas	FMCW
2FSK	499	0	0	0	0	0	0	0	0	0	0	0
P1	0	204	26	13	12	18	31	18	38	35	29	65
P2	0	10	226	9	13	17	64	17	25	105	21	12
P3	1	3	35	199	9	15	20	23	13	132	17	35
P4	0	14	51	15	66	19	26	52	31	136	49	58
Frank	0	12	35	8	5	97	48	23	22	135	32	77
T1	0	8	37	19	12	16	375	0	8	9	18	1
T2	0	4	20	16	6	9	14	390	7	7	2	1
T3	0	24	33	11	11	25	20	18	220	65	36	21
T4	0	10	37	13	11	19	22	9	17	351	1	0
Costas	0	10	15	6	10	7	10	4	10	9	428	7
FMCW	0	2	11	1	3	2	2	0	3	2	1	484

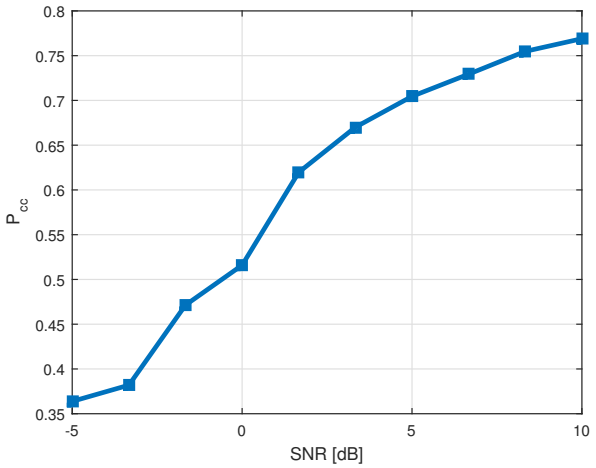

Fig. 3. Percent Correct Classification vs SNR

cannot easily cause a confusion between it an other signals. Lastly, the overall percent correct classification P_{cc} is plotted in 3. According to these results, if each of these signals are to have equal probability of being transmitted, then at 5 dB SNR it is expected that this could correctly classify the signal of interest at least 70% of the time.

V. CONCLUSIONS

Low probability of intercept (LPI) waveforms are in many modern radar systems to make detection by a potential adversary difficult. A variety of methods are used to accomplish this include frequency hopping and continuous pulsed waveforms. Our results show that polytime codes, polyphase codes, FSK, FMCW, Costas, and Frank codes, which are used are used to produce LPI signals can be classified using the spectral correlation density and support vector machines. At 0 dB SNR, at least a 50% correct classification among 12 different signals can be achieved. In many practical scenarios, such LPI signals may be monitored for several pulses if interception is the primary objective. Naturally, capturing more pulses will increase the probability of correct classification as several instances of the SCD can be used to classify the same signal. Therefore, these results show that LPI signals can be classified even in relatively low SNR (0 dB) or lower.

REFERENCES

[1] P. Pace, *Detecting and Classifying Low Probability of intercept radar*, 2nd ed. Norwood, MA, USA: Artech House, 2008, no. September.

[2] C. N. E. Persson, "Classification and Analysis of Low Probability of intercept radar Signals Using Image Processing," Master's thesis, Naval Postgraduate School, 2003.

[3] T. O. Gulum, "Autonomous Non-Linear Classification of LPI radar Signal Modulations," Master's thesis, Naval Postgraduate School, 2007.

[4] Y. Grishin and D. Janczak, "Computer-Aided Methods of the LPI Radar Signal Detection and Classification," vol. 6937, 2007.

[5] S. Haykin, D. J. Thomson, and J. Reed, *Spectrum Sensing for Cognitive Radio*, 2009, vol. 97, no. 5.

[6] H. Hu, J. Song, and Y. Wang, "Signal classification based on spectral correlation analysis and svm in cognitive radio," in *22nd International Conference on Advanced Information Networking and Applications*, March 2008, pp. 883–887.

[7] A. Fehske, J. Gaeddert, and J. Reed, "A New Approach to Signal Classification Using Spectral Correlation and Neural Networks," in *New Frontiers in Dynamic Spectrum Access Networks, 2005. DySPAN 2005. 2005 First IEEE International Symposium on*, Nov 2005, pp. 144–150.

[8] Q.-Q. Lu, M. Li, and X.-J. Wang, "Improved Method of Spectral Correlation Density and its Applications in Fault Diagnosis," *Beijing Keji Daxue Xuebao/Journal of University of Science and Technology Beijing*, vol. 35, no. 5, pp. 674–681, 2013.

[9] D.-S. Yoo, J. Lim, and M.-H. Kang, "ATSC Digital Television Signal Detection with Spectral Correlation Density," *Journal of Communications and Networks*, vol. 16, no. 6, pp. 600–612, 2014.

[10] Z.-B. Zhang, L.-P. Li, and X.-C. Xiao, "Detection and chip rate estimation of mpsk signals based on cyclic spectral density," *Xi Tong Gong Cheng Yu Dian Zi Ji Shu/Systems Engineering and Electronics*, vol. 27, no. 5, pp. 803–806, 2005.

[11] L. Zhu, H.-W. Cheng, and L.-N. Wu, "Identification of Digital Modulation Signals Based on Cyclic Spectral Density and Statistical Parameters," *Journal of Applied Sciences / Yingyong Kexue Xuebao*, vol. 27, no. 2, pp. 137–143, 2009.

[12] S. Image, "The Spectral Correlation Theory of Cyclostationary Series," vol. 11, pp. 13–36, 1986.

[13] R. Tibshirani, "Regression Selection and Shrinkage via the Lasso," pp. 267–288, 1994. [Online]. Available: http://citeseer.ist.psu.edu/viewdoc/summary?doi=10.1.1.35.7574

[14] B. E. Boser, I. M. Guyon, and V. N. Vapnik, "A Training Algorithm for Optimal Margin Classifiers," in *Proceedings of the Fifth Annual Workshop on Computational Learning Theory*, ser. COLT '92. New York, NY, USA: ACM, 1992, pp. 144–152. [Online]. Available: http://doi.acm.org/10.1145/130385.130401